Asian Journal of Atmospheric Environment
Vol. 8-2, pp. 96-107, June 2014
doi: http://dx.doi.org/10.5572/ajae.2014.8.2.096

Formation and Dispersion of Nitric Acid Vapor from Stack Flue Gas

Mi Jeong Park, Shi Chang Wu, Young Min Jo* and Young Koo Park[1)]

Department of Environmental Science and Engineering, Kyung Hee University, Gyeonggi-Do 446-701, Korea
[1)]Department of Environmental Engineering, Kangwon National University, Gangwon-Do 245-711, Korea

*Corresponding author. Tel: +82-10-7121-2485, E-mail: ymjo@khu.ac.kr

ABSTRACT

Extreme recovery of the thermal energy from the combustion of flue gas may bring about early gas condensation resulting in the increased formation of nitric acid vapor. The behavior of the nitric acid formed inside the stack and in the atmosphere was investigated through a computer-aided simulation in this study. Low temperatures led to high conversion rates of the nitrogen oxide to nitric acid, according to the Arrhenius relationship. Larger acid plumes could be formed with the cooled flue gas at 40℃ than the present exiting gas at 115℃. The acid vapor plume of 0.1 ppm extended to 25 m wide and 200 m high. The wind, which had a seasonal local average of 3 m/s, expanded the influencing area to 170 m along the ground level. Its tail stretched 50 m longer at 40℃ than at 115℃. The emission concentration of the acid vapor in the summer season was a little lower than in the winter. However, a warm atmosphere facilitated the Brownian motion of the discharged flue gas, finally leading to more vigorous dispersion.

Key words: Heat recovery, Nitric acid, Numerical simulation, Atmospheric reaction, Flue gas

1. INTRODUCTION

Currently, urban air pollution limits human activities outdoors and increases the cost of health care (Toronto Public Health, 2007). Industrial stacks are the primary emission sources that deteriorate air quality and waste the residual energy by releasing hot fluid. Therefore, the effective utilization and stringent management of energy sources are of great interest in Korea with regards to global energy issues. A combined heated and power plant attempts to take the thermal energy from the extreme heat of the exhausting flue gas (Wu *et al*., 2014). A low-temperature discharge can bring about less dispersion of the plume and pollutants.

Researchers have previously investigated the factors of flue gas dispersion, including the initial conditions of the exhaust gas, weather conditions, and environmental topography (Zhou *et al*., 2009). Table 1 briefly summarizes the emission conditions and practical models based on recent investigations. Most of the studies dealt with the NO_x flow in the atmosphere, but a few of them took into consideration the nitric acid formation based on the chemical reactions of NO_2. Once in the wet air, the production of nitric acid from NO_2 should also be considered. Acid rain arises from the oxidation of NO_2 in the troposphere that forms nitric acids, which are subsequently deposited on the earth's surface, either as precipitation or dry deposition. Nitric acid can easily be dissolved in the precipitation and contribute to local acid rain, which may cause the corrosion of structures as well as human health issues.

The test field in this study was a combined heated and power plant for electricity and steam generation in Ilsan, Korea. The plant uses liquefied natural gas (LNG) as its primary fuel. The exhausting stack gas temperature is 115℃ at 20.5 m/s and contains an average of 60 ppm NO. Prior to installing the practical heat recovery system, which reduced the flue gas temperature down to 40℃, we estimated the nitric acid concentration in the vicinity of the test area and its dispersion through numerical simulation in this study.

2. CHEMICAL CONVERSION TO NITRIC ACID

Nitric oxide and nitrogen dioxide, produced from the high temperature combustion of liquefied natural gas in a thermal power station, participate in a complex series of reactions in the atmosphere. One of the main reactions is the conversion of nitric oxide to nitrogen dioxide, as follows:

$$2NO + O_2 \rightarrow 2NO_2 \quad (1)$$

This overall reaction has been widely studied and con-

Table 1. Mathematical modeling studies of gas emission.

Authors	Emission types	Dispersion model types
Lateb, M. (2011)	Building roof stacks: pollutants	Realizable k-ε turbulence model: the distribution of pollutant concentrations with stack height and exhaust velocity
Cretu, M. (2010)	Incinerator and thermal power station stacks: NO_x, SO_2, and CO	Gaussian plume dispersion model: pollutant concentration maps with wind direction
FreddyKho, W.L. (2007)	Diesel power plant stacks: NO_2 and SO_2	ISC-AERMOD dispersion model: pollutant dispersion by wind direction and ground-level concentration
Yousif, S.A. (2006)	Gas power station stacks: NO_x, SO_2, and PM	Gaussian plume model: ground-level concentrations of pollutants
Brown, G.J. (2005)	Alumina refinery calciner stacks: odor	CFX-5 code: ground-level odor through multi-flue stack

firmed under various environmental conditions (Morrion *et al.*, 1996). According to a kinetic study, the conversion of NO to NO_2 is inversely proportional to the absolute temperature due to the negative activation energy (Baulch *et al.*, 1973).

Nitrogen dioxide and water vapor react in the gas phase to form nitric acid vapor and nitric oxide, as follows:

$$3NO_2+H_2O \rightarrow NO+2HNO_3 \quad (2)$$

The following reactions are proposed to describe the above reaction (England and Corcoran, 1974):

$$2NO_2+H_2O \rightarrow HNO_2+2HNO_3 \text{ (slow)} \quad (3)$$

$$2HNO_2 \rightarrow H_2O+NO+NO_2 \text{ (fast)} \quad (4)$$

The gas-phase reaction of nitrogen dioxide with water vapor is a homogeneous reaction that initially follows third-order kinetics, according to the following equation (5):

$$R_{HNO_3} = -k\,[NO_2]_2\,(H_2O) \quad (5)$$

where R_{HNO_3} represents the rate of production of nitric acid, and k is the Arrhenius constant dependent on the activation energy and operating temperature. The activation energy of the reaction was found to be approximately −978 cal (England and Corcoran, 1974). The final obtained value of the reaction rate, k, was $5.5 \times 10^4\,L^2mol^{-2}sec^{-1}$ at 25°C. The reaction of the part-per-million concentrations of nitric oxide with large excesses of both oxygen and water vapor were examined. As a result, the concentrations of the latter two compounds did not change significantly during the reactions (England and Corcoran, 1975). In addition, the decomposition of nitric acid vapor at low pressures was found to be very slow at ordinary temperatures and, therefore, it was not considered to be an influencing factor in the system (Johnston *et al.*, 1951).

3. NUMERICAL CALCULATION

3. 1 Computational Model

In this study, we examined a combined heated and power plant for the generation of both electricity and steam in Ilsan, Korea. The site is in a highly populated residential area that includes apartments and office buildings near the plant, as shown in the map in Fig. 1(a). A 41-m-high hill is situated upstream of the stack and a subway station is located 450 m to the southeast. The model shown in Fig. 1(b) was created by Gambit Software and matches the map. The model domain was designed to be 2,000 m by 1,000 m in a plane and 300 m in height. A triangular cell was chosen for the ground face, hexahedral-based mesh was used for the cylinder shape, and tetrahedral-based mesh was adopted for the domain. We hypothesized that a total of 1.2 million gradient meshes were sufficient for the composition of the ground.

The standard κ~ε turbulent model based on the eddy viscosity hypothesis was used for the pollutant dispersion (Konig and Mokhtarzadeh-Dehghan, 2002). It is a semi-empirical model composed of transport equations for the turbulence kinetic energy (κ) and its dissipation rate (ε). The κ~ε model was derived with the assumptions that the flow is fully turbulent and the effects of the molecular viscosity are negligible. The governing equations of the fluid flow (mass, momentum, and energy equations) represent mathematical statements of the conservation laws of physics: the law of mass conservation, Newton's second law, and the first law of thermodynamics. The Navier-Stokes equation solves the viscous stress term, which is unknown within the governing equations (Versteeg and Malalasekera, 1995). In this study, the chemical conversion of nitric oxide to nitric acid was simulated on the basis of volume. The solver, SIMPLE, suggested by Patankar and Spalding (1972), discretized the equations of momentum and continuity.

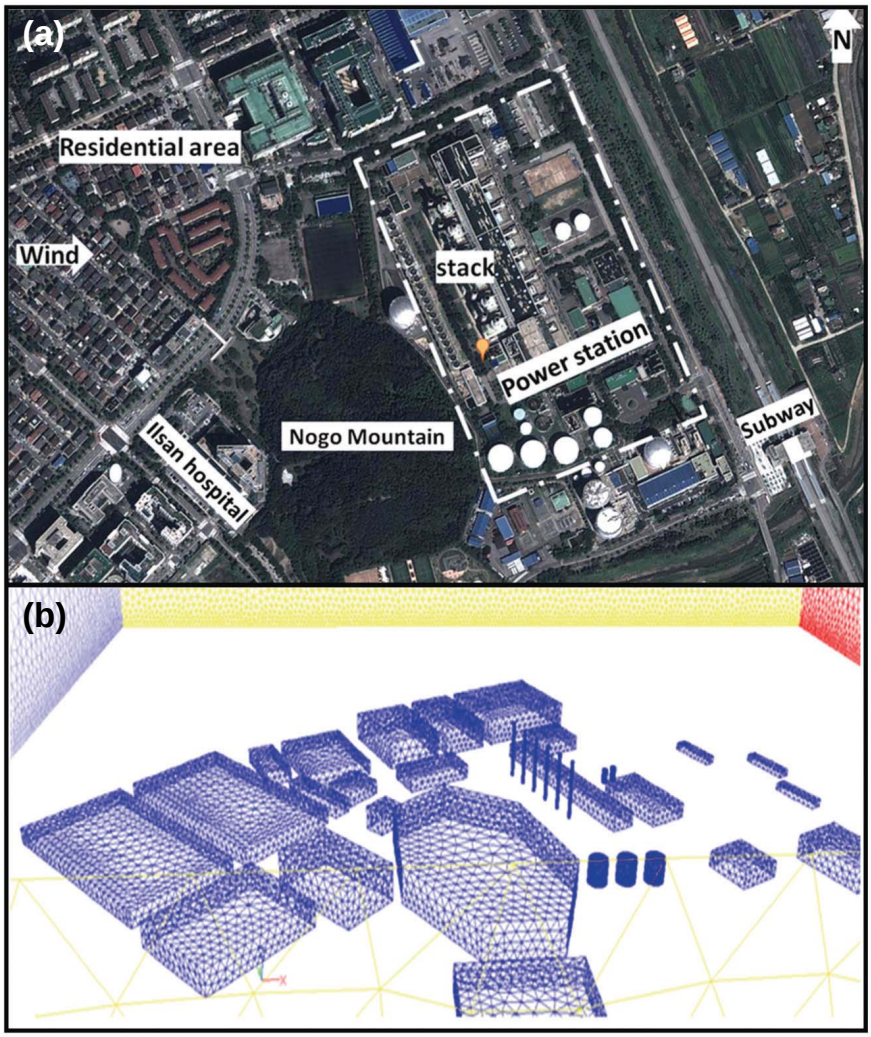

Fig. 1. Geographic model of the test power station: (a) local map and (b) mesh modeling.

3. 2 Meteorological Conditions

The annual wind rose on the test field from 2010 to 2012 is presented in Fig. 2(a). The prevailing wind direction was eastward with an average wind speed of 3 m/s. The velocity profile of the wind followed the principle of increasing with altitude, as defined by Deacon's equation, Eq. (6) (Peterson and Hennesse, 1977),

$$U_Z = U_{ref} \cdot \left(\frac{Z}{Z_{ref}}\right)\alpha \quad (6)$$

where the wind speed, U_{ref}, corresponds to Z_{ref}, which was 3 m/s at 10-m-high, and α indicates the constant of the atmospheric stability, which was 0.2 in this study based on the weak instability of the atmospheric situation in the urban area (Irwin, 1979). The vertical temperature gradient was applied in order to estimate the plume rise according to the atmospheric conditions, as shown in the following Eq. (7),

$$T = T_0 - 6*H \quad (7)$$

where T_0 is the ground temperature (°C) and H is the altitude (km). Ilsan has four distinctive seasons in the air temperature. Table 2 lists the average temperature of the day and night in 2012. The maximum and minimum air temperature at the field site reached 35.7°C in the summer and −17.4°C in the winter, respectively. From the present meteorological background, the gradient profiles of the air temperature and wind speed were calculated and are described in Fig. 2(b).

4. RESULTS AND DISCUSSION

In the present study, the formation and dispersion of nitric acid were investigated by numerical simula-

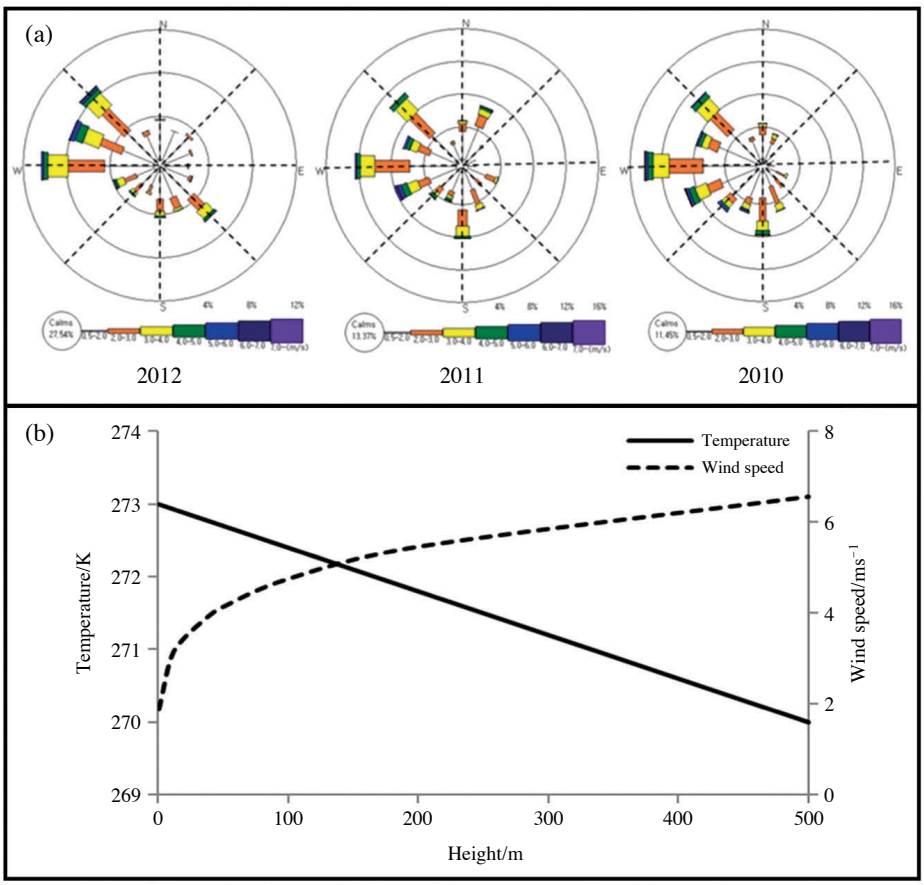

Fig. 2. Meteorological conditions: (a) wind rose; (b) lapse rate of the air temperature ($T_{initial}$=20°C) and vertical gradient of the wind speed in the test area.

Table 2. Day-night temperature variation and average of the four seasons in 2012 in Ilsan.

	Spring/°C	Summer/°C	Autumn/°C	Winter/°C
Day (max)	22.9	35.7	19.9	−9.1
Night (min)	6.6	26.5	8.9	−17.4
Average	12.1	30.9	13.5	−13.5

tion as summarized in Table 3, and discussed mainly in terms of the gas temperature, the emission concentration of NO, and the wind speed.

4. 1 Formation of Nitric Acid from Flue Gas

In practice, the discharged NO_2 may form acid mist in a humid atmosphere. A typical gas phase reaction of NO_2 with the water vapor from flue gas or atmospheric moisture is homogeneous and initially follows third-order kinetics (Goyer, 1963). The intermediates of the serial reactions are dinitrogen tetroxide (N_2O_4) and nitrous acid (HNO_2), which have very short lifetimes. The presence of oxygen does not change the initial reaction rate, but instead promotes the equilibrium of the reaction. The reaction extent is critically dependent on the temperature: the lower the temperature, the greater the production of nitric acid (England and Corcoran, 1974).

4. 1. 1 Effects of the Flue Gas Temperature

The conversion of NO_x to nitric acid within the stack varies with the temperature inside. Fig. 3 shows the concentration profiles of the nitric acid mist at the downflow of the stack with the flue gas temperature. The inner figures (a2, b2) indicate the formation along the center of the stack. The stack inlet concentration of the nitric oxide was assumed to be 60 ppm, which was the average value released from the test power plant. Obviously, a larger plume of acid mist was found at a flue gas temperature of 40°C rather than 115°C. The greatest amount of nitric acid was found at the stack exit, and the concentration contour for 0.1 ppm rose up to 200 m in height and 50 m in width at 40°C, while it reached about 180-m-high and 40-m-wide for a flue gas temperature of 115°C. The dilution rate

Table 3. Boundary conditions for the model calculation.

Boundary condition		Dispersion	Reaction
Ambient	Wind speed	0, 1 m/s, 3 m/s, 5 m/s, 10 m/s	
	Temperature	−20°C, 0°C, 20°C, 35°C	
	Humidity	10%, 20%, 40%, 60%	
Flue gas	Velocity	10 m/s, 15 m/s, 20.5 m/s, 25 m/s	
	Temperature	40°C, 70°C, 100°C, 115°C	
	Species	H_2O, O_2, N_2, NO, NO_2	H_2O, O_2, N_2, NO, NO_2, HNO_3
Modeling	Viscous model	Standard κ~ε model	
	Governing equation	Multiple species transport	Volumetric reaction
		Transport equation	Chemical reaction equation
	Variable	Diffusivity	Reaction rate
	Constant	Lennard-Jones parameters	Rate constant

should be more significant for the formation of nitric acid contours in the atmosphere than the reaction rate. As can be seen in the inside figure (a2), the acid concentration approaches 3.6 ppm at the upper side of the stack. Therefore, it is possible that the acid vapor is condensed as soon as it contacts the cold air outside. Then, it can seriously impact the stack structure as well as deteriorate the visual appearance. Therefore, the use of corrosion-resistant materials is essential for the stack inner shell when the stack gas is cooled.

4. 1. 2 Effects of the Initial Concentration of Nitric Oxide

The initial amount of NO in the flue gas is directly related to the production of nitric acid. As presented above, nitric oxide converts to nitric dioxide in an oxygen-sufficient atmosphere, and some of the nitric dioxide then becomes nitric acid with the presence of the water moisture. Fig. 4 shows the nitric acid concentration contours with initial NO concentrations of 10 ppm, 50 ppm, 60 ppm, and 100 ppm, which are the target concentrations of the power plant by the new facility, the new national emission standard, the present emission average, and the standard for old facilities, respectively.

Increased amounts of nitric acid were formed with 100 ppm of NO, while a very slender plume body was generated with 10 ppm of NO. From Eq. (5), the production rate of HNO_3 is directly proportional to the NO_2 concentration in the second order, while the NO_2 formation also depends on the NO concentration in the second order (Morrion *et al.*, 1996). In particular, the NO concentration, rather than those of the oxygen and water vapor, directly determines the reaction rate for part-per-million level reactions. As observed in Fig. 4, the inner contours, indicating a high level of nitric acid close to the stack outlet, are more clearly growing with NO concentration of the flue gas. However, the outside contour of 0.1 ppm has not been expanded very much, which implies the significance of atmospheric dilution. The mixing with a large volume of air instantaneously reduces the acid concentration to lower than 0.1 ppm.

Fig. 5 summarizes the HNO_3 concentration variations along the stack center with four initial concentrations. The reaction was initiated even from the stack bottom and then increased exponentially as it rose up through the stack. Upon reaching the maximum level at the top of the stack, the flue gas began to dilute with fresh air, showing a steep decrease in the acid level. At a height greater than 250 m, an obvious acid level could no longer be seen. The predictions in Fig. 4 and Fig. 5 were calculated based on the conditions of no wind and no background nitric acid. In such a case, downwash of the flue gas including nitric acid vapor was not observed. Therefore, it can be concluded that there was no direct impact of the acidic atmosphere on the ground near the emission source.

4. 2 Dispersion of Acid Vapor in the Atmosphere

The vertical momentum and horizontal wind cause the discharged flue gas to rise up and to disperse into the air. The flue gas penetrates into a large body of air more quickly on windy days, leading to the efficient dilution of pollutants. The distribution pattern of the pollutants and its influencing area were estimated in the area adjacent to the test power plant.

4. 2. 1 Nitric Acid Concentration Distribution in the Atmosphere

The discharged flue gas is dispersed into the ambi-

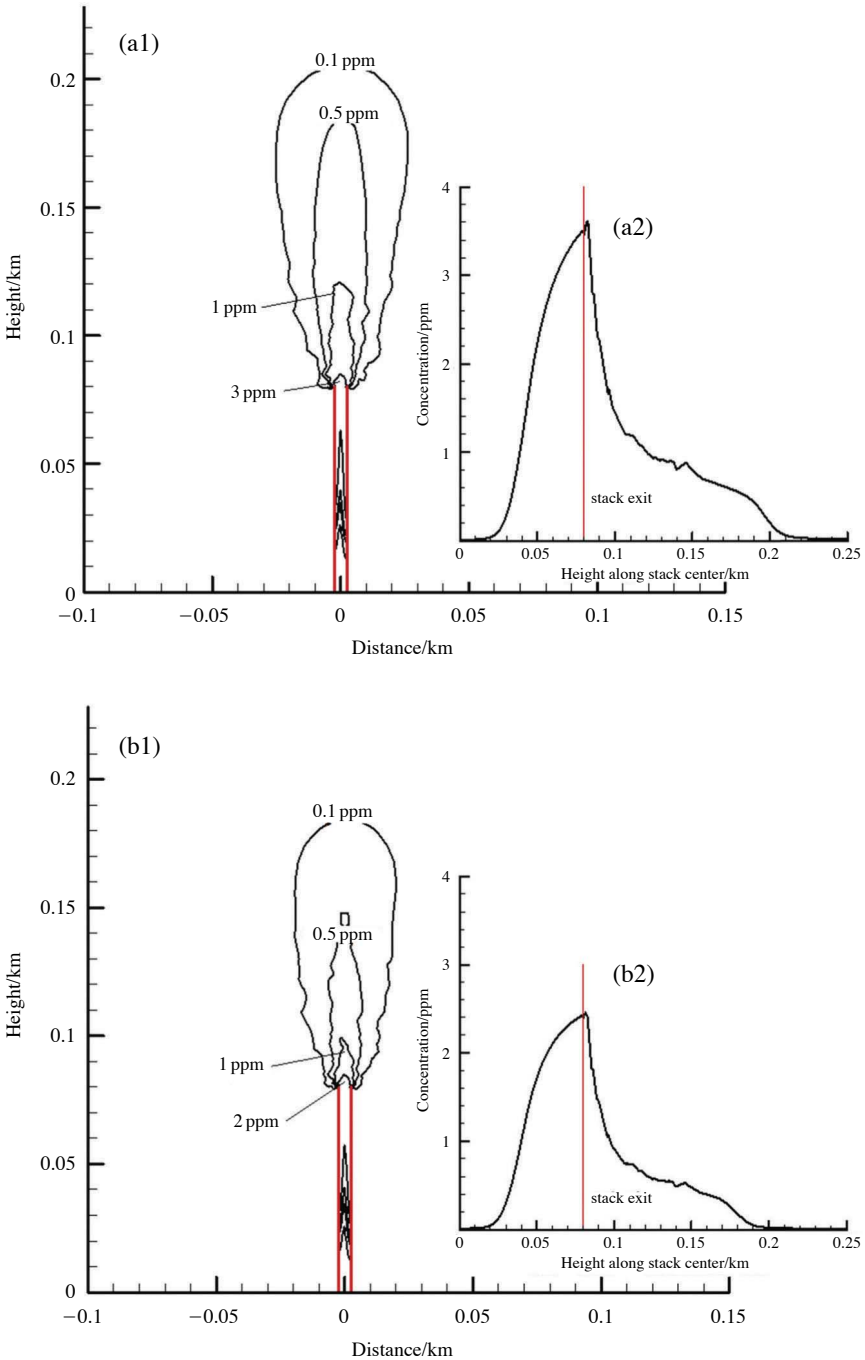

Fig. 3. Vertical concentration profiles of the nitric acid mist with the flue gas temperature: (a) 40°C; (b) 115°C (supplementary figures (a2, b2) show the vertical distribution of the nitric acid concentration along the stack center-line).

ent air in three dimensions: the downwind (x-axis), crosswise (y-axis), and longitudinal (z-axis) directions as described in Fig. 6. The wind flows to the east (from left to right in Fig. 6(a)) at 1 m/s. In Fig. 6(a), the acid concentrations reach their peak values at certain distances from the emission source stack. For example, the maximum concentration at an 80 m height from the ground was found at a distance of 180 m from the stack. In this study, we focused on the low level altitude in order to investigate the human effects on the ground. Despite some difference in the acid concentration near the stack with altitude, it approached cer-

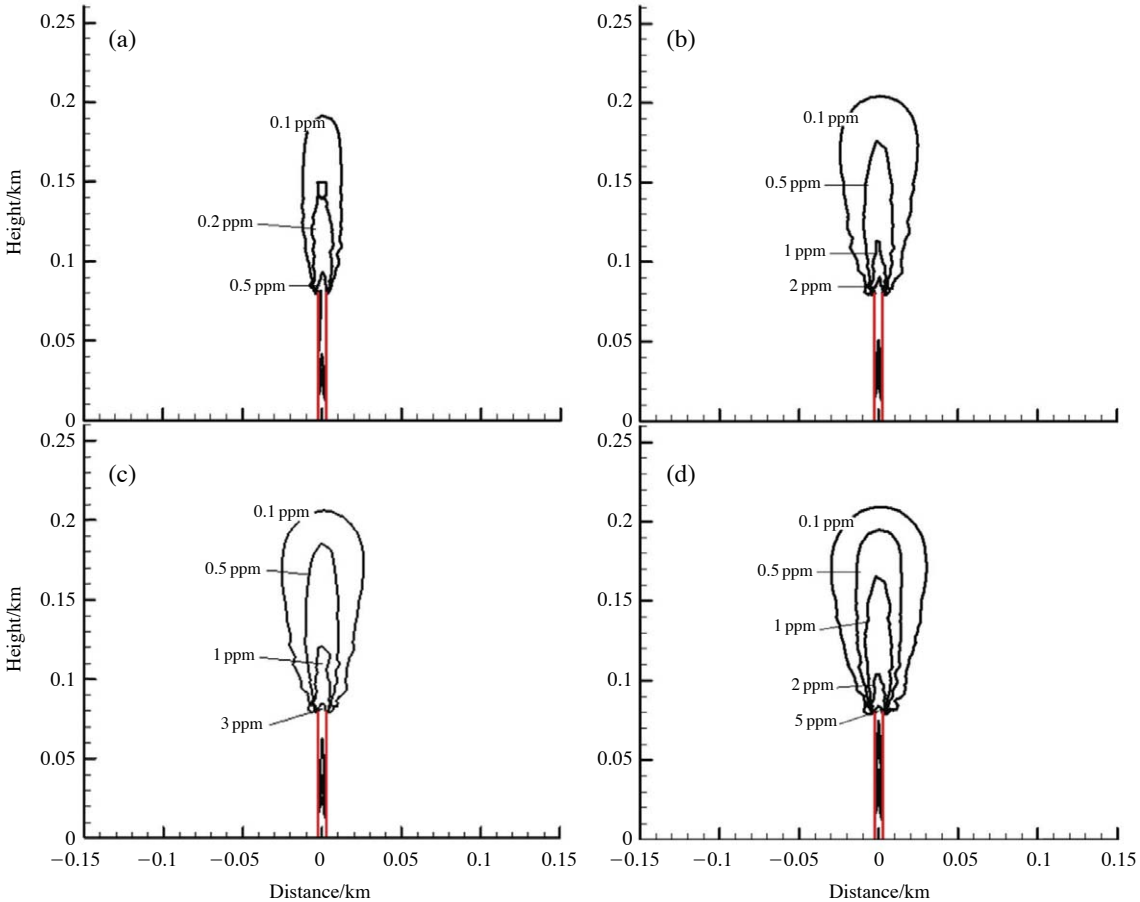

Fig. 4. HNO_3 concentration contours with the NO concentration on windless days: (a) 10 ppm; (b) 50 ppm; (c) 60 ppm; and (d) 100 ppm.

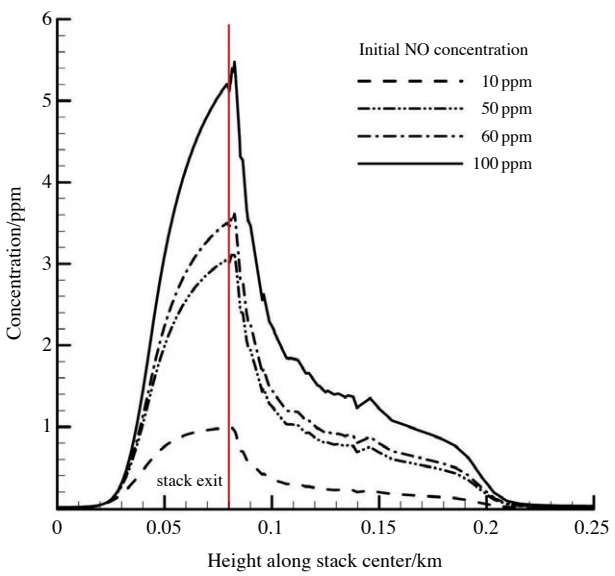

Fig. 5. HNO_3 concentration variations along the stack center in terms of the initial NO concentration.

tain levels over 400 m or 450 m; approximately 6 ppb for 40°C and below 4 ppb for 115°C. In other words, a thick band of higher acid levels at 40°C propagates a long distance. The altitude indicating the ground level, 1.5 m, could have an acid impact by flue gas emissions in quite a large area, particularly with 7 ppb at 40°C and 3.5 ppb at 115°C. These values are quite noticeable comparing to the field measurement which was detected at less than 1.2 ppb.

Fig. 6(b) represents the nitric acid concentration in the crosswise direction, namely, the y-axis direction, with different altitudes at x=200 m. The profiles demonstrate that the distribution from and to the rear of the stack is a Gaussian pattern, which indicates that there is not a significant influence due to wind shifting, but that there are differences according to altitude. This implies that there are only effects from natural diffusion and dilution without any direct wind effects.

In the longitudinal direction (the same as the z-axis, shown in Fig. 6(c)), the distribution trends also followed a Gaussian distribution with the height. The

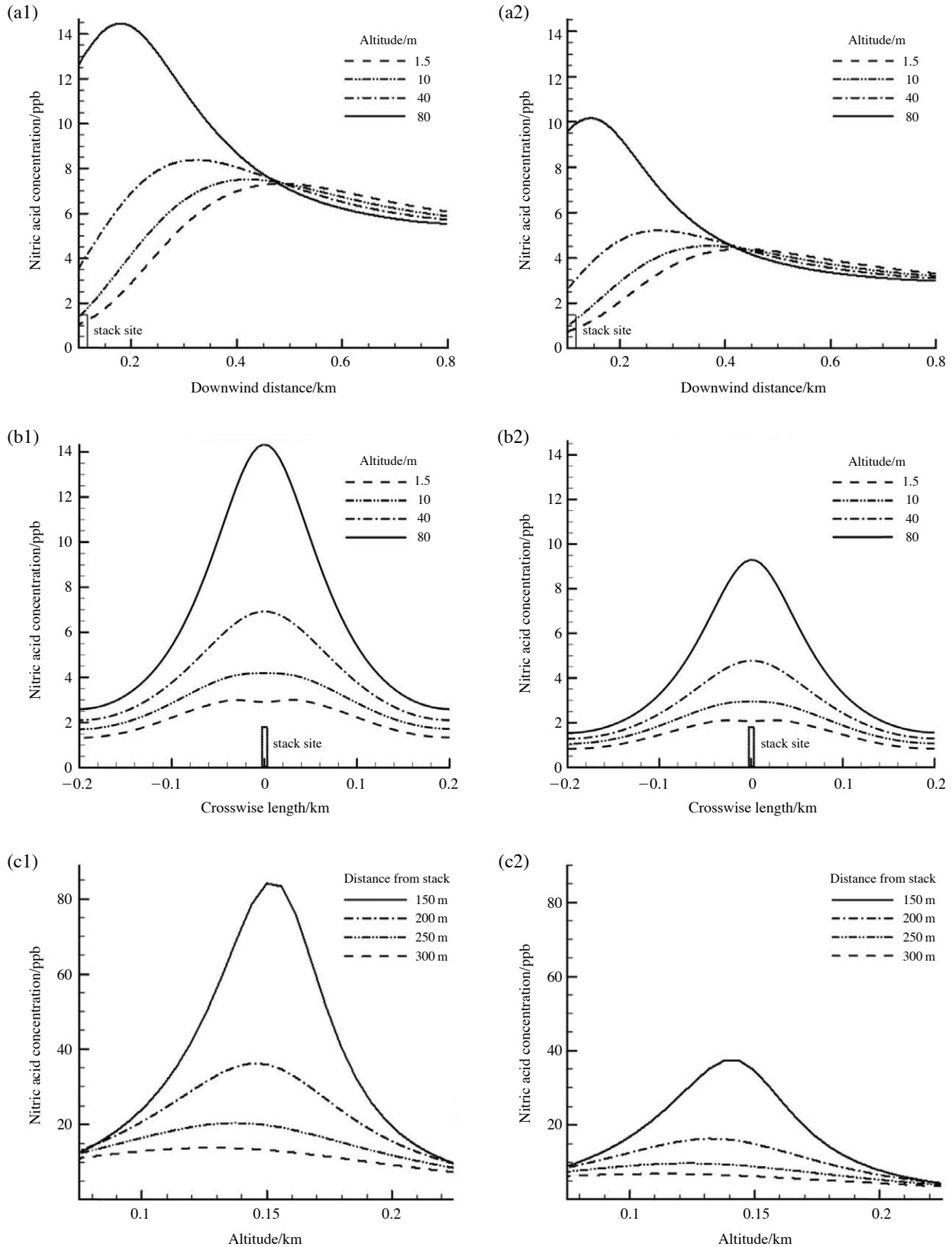

Fig. 6. 3-D concentration profiles for (1) 40°C and (2) 115°C flue gas with wind speed of 1 m/s: (a) downwind-x-axis; (b) crosswise-y-axis; and (c) longitudinal-z-axis.

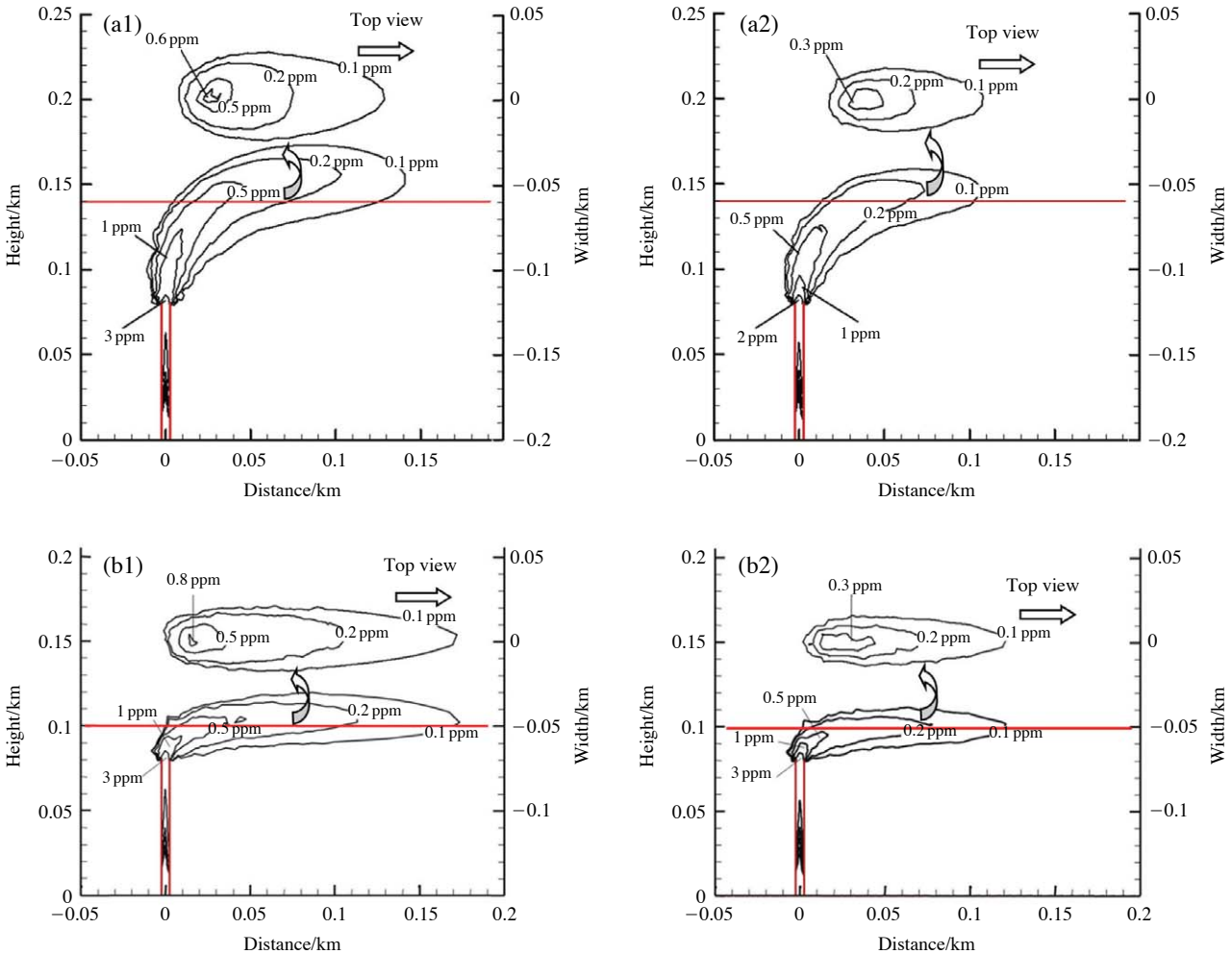

Fig. 7. Dispersion of HNO_3 vapor with wind speed and flue gas temperature: (a1) 1 m/s wind, 40°C; (a2) 1 m/s wind, 115°C; (b1) 3 m/s wind, 40°C; and (b2) 3 m/s wind, 115°C.

maximum peaks were found at 150 m and 140 m high for 40°C and 115°C, respectively. As shown in Fig. 6(a), the concentration peaks were at approximately 150 m to 140 m away from the stack. Buoyancy due to warm flue flow promotes greater lifting up of the acid plume body and, therefore, touches the peak at approximately 150 m high rather than 80 m from the stack outlet. Buoyancy also facilitates the formation reaction of nitric acid as it is floating up.

4. 2. 2 Effects of Wind Speed

Wind is one of the key factors causing atmospheric turbulence. The most frequently occurring wind speed in the test area was 3 m/s at the top of the stack. As seen in Fig. 7, faster winds caused flatter plumes that extended further, particularly at low temperatures. The influencing area of 0.1 ppm HNO_3 with a 3 m/s wind was an ellipsoid with 170 m length, 40 m width, and 40 m thickness at a flue gas temperature of 40°C (b1), which was 50 m longer than that at 115°C (b2). Low speed winds formed larger and higher acid plumes (a1, a2), but influenced a shorter distance (120-140 m) windward. The plume width as seen from the top view (50 m) was also wider at 40°C than at 115°C (35 m) for the wind speed of 1 m/s. Therefore, low temperature flue gas in a light wind may more significantly affect the environment in the vicinity of the emission source.

4. 2. 3 Seasonal Variation of the Acid Concentration

As summarized in Table 2, the test area, Ilsan, had distinctive weather conditions throughout the seasonal variation, for the air temperature in particular.

Fig. 8 presents the HNO_3 concentration curves along the stack center as a function of the outside air temperature without wind: −15°C, 0°C, 15°C, and 30°C. The concentration of the stack inside up to a height of 80 m was almost overlapped due to no direct contact with the atmosphere. As was the case close to the stack

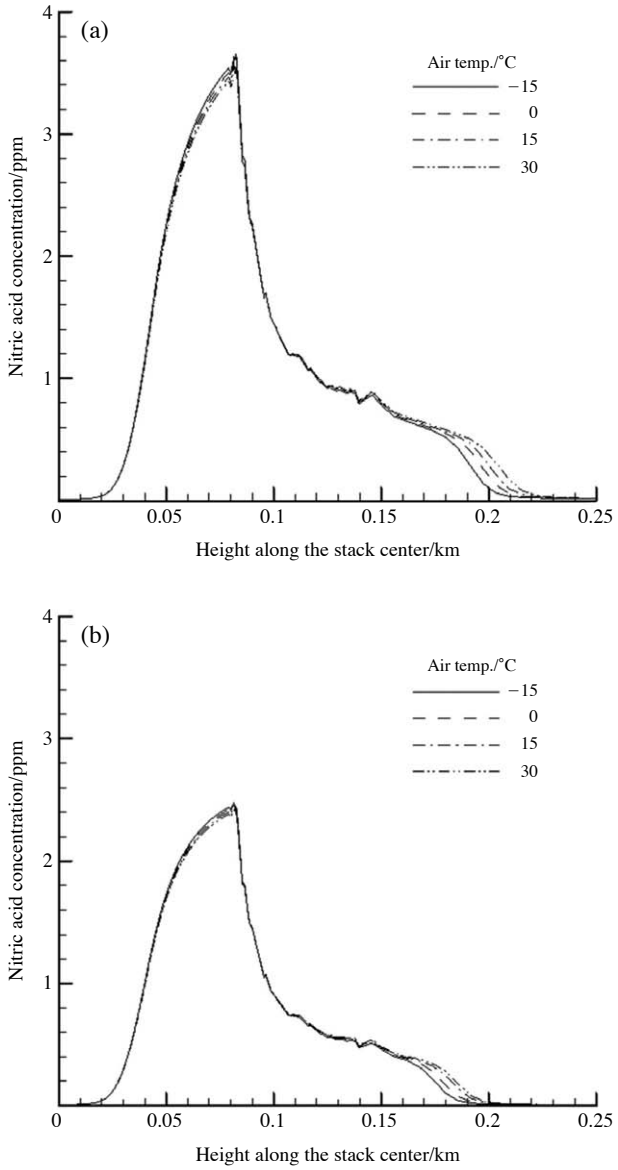

Fig. 8. Longitudinal concentration distribution along the stack center of the flue gas in terms of air temperature: (a) 40°C and (b) 115°C.

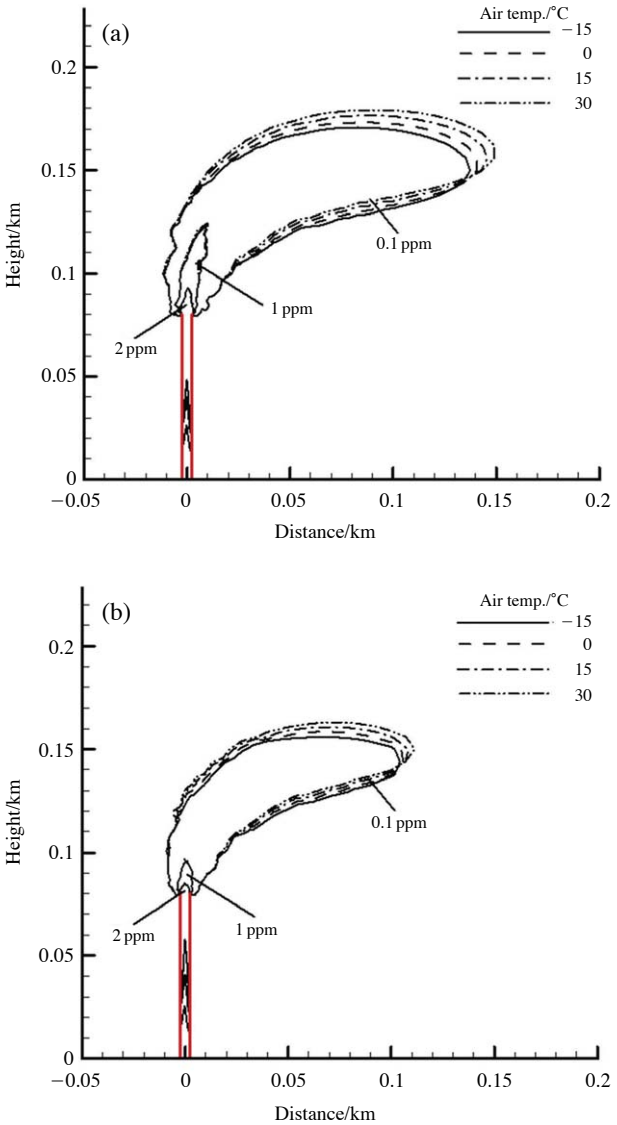

Fig. 9. HNO_3 concentration contours in different seasonal condition at 1 m/s wind speed with flue gas temperatures of: (a) 40°C and (b) 115°C.

topside, external conditions may affect the reaction even inside of the stack. The acid level dropped steeply directly after exiting the stack, probably due to dilution. The effects of the air temperature were more significant at high temperatures, as clearly indicated by the data from approximately 160-m-high. Consequently, the seasonal variation of the acid plume formation would not be very large, at least in the range of −15°C to 30°C. The absolute value of the concentration depends on the flue gas temperature instead.

On the other hand, the concentration profiles with a wind speed of 1 m/s are displayed in Fig. 9. A typical summer day at 30°C shows little further dispersion of the acid plume. Hot weather may lead to more active Brownian motion of the gas molecules, resulting in wide scattering. However, although it predicted an obvious tendency with the air temperature, the difference between the seasons was not as significant as the plume size growth by flue gas cooling to 40°C.

5. CONCLUSIONS

From the point of energy savings, the recovery of the internal heat of stack flue gas using high efficiency

heat exchangers has been attempted. However, extreme recovery of thermal energy may reduce the exiting temperature, possibly resulting in low buoyancy and less dilution effects. In particular, cooled flue gas includes high moisture content and may produce higher amounts of nitric acid depending on the environmental conditions. Therefore, we estimated the quantitative formation of the acid plume and its dispersion by mathematical computations in this study. As a result of the calculations, the following evaluations could be obtained:

(1) NO_2 formed from the flue gas produces a nitric acid mist with the aid of the moisture in the stack and the humid air outside. The acid plume size was larger for the cooled flue gas (40°C), whose size could be expanded to 25 m in width and 200 m in height for a 0.1-ppm HNO_3 level. It was obviously larger in winter.
(2) The direct influencing distance as well as the absolute concentration of nitric acid were more significant at 40°C than at 115°C due to less Brownian motion.
(3) At the distance of 800 m from the stack, the acid still presented at approximately 6 ppb for 40°C and 3.5 ppb for 115°C. The Gaussian distribution of the HNO_3 concentration was presented in the crosswise and longitudinal directions.
(4) While the influencing area of the acid vapor at low wind speeds could be limited to near the stack, high-speed winds stretched the acid plume to long distances, depending on the flue gas temperature.
(5) Consequently, plume size would be determined by the flue gas temperature rather than by the outside air temperature.

ACKNOWLEDGEMENT

This work was supported by a grant from the Power Generation & Electricity Delivery Program of the Korea Institute of Energy Technology Evaluation and Planning (KETEP), funded by the Korean government Ministry of Knowledge Economy (2011T100200186).

REFERENCES

Baulch, D.L., Drysdale, D.D., Horne, D.G. (1973) Evaluated Kinetic Data for High Temperature Reactions, Vol.2, Homogeneous Gas Phase Reactions of the H_2-N_2-O_2 System, London, pp. 285-300.

Brown, G.J., Fletcher, D.F. (2005) CFD prediction of ddour dispersion and plume visibility for alumina refinery calciner stacks. Process Safety Environment 83(B3), 231-241.

Cretu, M., Teleaba, V., Ionescu, S., Ionescu, A. (2010) Case study on pollution prediction through atmospheric dispersion modeling. Recent advances in mathematics and computers in business, economics biology & chemistry, pp. 122-127.

England, C., Corcoran, H.W. (1974) Kinetics and mechanisms of the gas-phase reaction of water vapor and nitrogen dioxide. Industrial and Engineering Chemistry Fundamentals 13(4), 373-384.

England, C., Corcoran, H.W. (1975) The rate and mechanism of the air oxidation of parts-per-million concentration of nitric oxide in the presence of water vapor. Industrial and Engineering Chemistry Fundamentals 14(1), 55-62.

Freddy, W.L., Sentian, J., Radojevic, M., Tan, C.L., Halipah, S. (2007) Computer simulated versus observed NO_2 and SO_2 emitted from elevated point source complex. International Journal of Environment Science and Technology 4, 215-222.

Goyer, G.G. (1963) The formation of nitric acid mist. Journal of Colloid Science 19, 616-624.

Irwin, J.S. (1979) Estimating plume dispersion-A recommended generalized scheme, in Preprints of Fourth Symposium on Turbulence, Diffusion and Air Pollution, American Meteorological Society, pp. 62-69.

Johnston, H.S., Foering, L., Tao, Y.S., Messerly, G.H. (1951) The kinetics of the thermal decomposition of nitric acid vapor. Journal of the American Chemical Society 73(5), 2319-2321.

König, C.S., Mokhtarzadeh-Dehghan, M.R. (2002) Numerical study of buoyant plumes from a multi-flue chimney released into an atmospheric boundary layer. Atmospheric Environment 36, 3951-3962.

Lateb, M., Masson, C., Stathopoulos, T., Bedard, C. (2011) Effect of stack height and exhaust velocity on pollutant dispersion in the wake of a building. Atmospheric Environment 45, 5150-5163.

Morrion, M.E., Rinker, R.G., Corcoran, W.H. (1996) Rate and mechanism of gas-phase oxidation of parts-per-million concentrations of nitric oxide. Industrial Engineering and Chemical Fundamentals 5, 175-181.

Patankar, S.V., Spalding, D.B. (1972) A calculation procedure for heat, mass and momentum transfer in three-dimensional parabolic flows. International Journal of Heat & Mass Transfer 15, 1787-1806.

Peterson, E.W., Hennesse, J.P. (1977) On the use of power laws for estimates of wind power potential. Journal of Applied Meteology 17, 390-395.

Toronto Public Health (2007) Air pollution burden of illness from traffic in Toronto, problems and solutions.

Versteeg, H.K., Malalasekera, W. (2007) An Introduction to Computational Fluid Dynamics, the Finite Volume Method (Second Edition). Longman, New York, pp. 1-38.

Wu, S.C., Jo, Y.M., Park, Y.K. (2014) Effect of heat recovery from flue gas on the local humidity and NO_x dispersion in a thermal power station. Aerosol and Air

Quality Research 14, 840-849.
Yousif, S.A., Salem, A.A., Nassar, Y.F., Bader, I.F. (2006) Investigation of pollutants dispersion from power stations. International Journal of Energy Research 30, 1352-1362.
Zhou, X.P., Yang, J.K., Ochieng, R.M. (2009) Numerical investigation of a plume from a power generating solar chimney in an atmospheric cross flow. Atmospheric Research 91, 26-35.

(Received 25 March 2014, revised 20 May 2014, accepted 2 June 2014)